Production cross sections of superheavy elements $Z = 119$ and 120 in hot fusion reactions

Long Zhu,[1,2] Wen-Jie Xie,[1,2] and Feng-Shou Zhang[1,2,3,*]

[1]*College of Nuclear Science and Technology, Beijing Normal University, 100875 Beijing, China*

[2]*Beijing Radiation Center, Beijing 100875, China*

[3]*Center of Theoretical Nuclear Physics, National Laboratory of Heavy Ion Accelerator of Lanzhou, Lanzhou 730000, China*

(Received 30 November 2013; revised manuscript received 7 February 2014; published 24 February 2014)

The production cross sections of superheavy nuclei in hot fusion reactions are investigated systematically. In hot fusion reactions, the capture cross section can be obtained by calculating the weighted average of the transmission probability for different orientations of deformed colliding nuclei. An analytical formula for calculating the value of the fusion probability is proposed, which is suitable for both hot and cold fusion reactions. The orientation effects are considered empirically in calculating the fusion probability. The method proposed in the present work reproduces the measured evaporation residue (ER) cross sections in hot fusion reactions acceptably well. The formula also gives reasonable results for fusion probability in cold fusion reactions. Using this method the evaporation residue cross sections for synthesizing $Z = 119$ and 120 are predicted. It is found that for hot fusion reaction's larger maximal ER cross section of the $4n$ channel corresponds to lower optimal incident energy.

DOI: 10.1103/PhysRevC.89.024615 PACS number(s): 25.70.Mn, 25.70.Pq, 24.10.Lx, 27.90.+b

I. INTRODUCTION

The synthesis of superheavy elements (SHEs) is an outstanding research field. In recent decades, much experimental progress has been made in synthesizing SHEs. The syntheses of the SHEs with $Z \leqslant 112$ by using cold fusion reactions based on ^{208}Pb and ^{209}Bi [1] and with $Z = 112$ to 118 by hot fusion reactions of ^{48}Ca with actinide targets [2–7] have been reported. The element $Z = 113$ was synthesized by the RIKEN group in the cold fusion reaction $^{70}\mathrm{Zn} + ^{209}\mathrm{Bi}$ with a cross section value equal to some percent of a picobarn [8]. It is difficult to produce heavier nuclei with $Z \geqslant 113$ in cold fusion reactions because of the very small production cross sections. Many theoretical works [9–22] have been done to investigate the synthesis mechanism of superheavy nuclei (SHN).

The evaporation residue (ER) cross section is very small, which strongly depends on beam energy and the combination of projectile and target. Therefore, finding favorable reactions and the optimal beam energy range are very important for synthesis of SHEs.

The process of the calculation of the ER cross section can be divided into three steps. The first step is that the capture barrier must be overcome and a dinuclear system is formed. The second step is two touched nuclei fusing together to a compound nucleus. Finally, the compound nucleus loses its excitation energy by the emission of particles and γ rays to reach its ground state. The ER cross section can be written as [9]

$$\sigma_{\mathrm{ER}} = \sigma_{\mathrm{cap}} P_{\mathrm{CN}} W_{\mathrm{sur}}, \tag{1}$$

where σ_{cap}, P_{CN}, and W_{sur} are capture cross section, fusion probability to compound nucleus, and survival probability of the excited compound nucleus, respectively. The capture cross section is usually calculated by using an empirical coupled-channel model [10], in which the barrier distribution function method is introduced. The survival probability W_{sur} of the compound nucleus against fission in the de-excitation process is considered as one of the crucial factors for producing SHN, which is often analyzed by using statistical models. Unlike the first and third steps, the process of the second step is quite unclear. Many approaches [11–16] are used to calculate the value of P_{CN} including empirical formulas [17–19]. The predicted optimal ER cross sections and corresponding incident energies from different models are quite different for synthesis of SHEs with $Z = 119$ and 120.

In this work, the hot fusion reactions for producing SHN with $Z \geqslant 112$ are studied. The capture cross section can be obtained by calculating weighted average transmission probability for different orientations of deformed nuclei. We study the influence of some physical quantities on fusion probability and propose a reasonable formula to calculate P_{CN}. The survival probability of the compound nuclei is described with the HIVAP code [23,24]. The aim of this paper is to study the influence of some physical quantities on fusion probability and to propose a reasonable method to analyze the production cross sections of SHEs $Z = 119$ and 120.

The article is organized as follows. In Sec. II, we describe the way of calculating capture cross section and propose a formula for calculating the value of P_{CN}. The results and discussion are presented in Sec. III. We summarize the main results in Sec. IV.

II. METHOD DESCRIPTION

In fusion reactions involving deformed nuclei, the fusion barrier distributions are dominated by the deformation effects [25,26]. In hot fusion reactions, the targets have large prolate deformation. Therefore, the capture cross section for two deformed colliding nuclei can be written as

$$\sigma_{\mathrm{cap}}(E_{\mathrm{c.m.}}) = \frac{1}{4}\int_0^{\pi} \sin\theta_1\, d\theta_1 \int_0^{\pi} \sigma_{\mathrm{cap}}(E_{\mathrm{c.m.}},\theta_1,\theta_2)\sin\theta_2\, d\theta_2. \tag{2}$$

where 1 and 2 denote the projectile and target, respectively. $\theta_{1,2}$ are the angles between the symmetry axis of the deformed nuclei and the collision axis. $E_{\mathrm{c.m.}}$ is the bombarding energy in

*fszhang@bnu.edu.cn

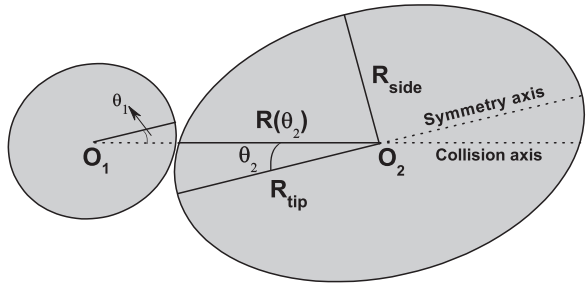

FIG. 1. Fusionlike shape parametrization for two ellipsoidal nuclei.

the center-of-mass system. A typical fusionlike configuration of ellipsoidal target and projectile nuclei can be seen in Fig. 1. The $\sigma_{\rm cap}(E_{\rm c.m.},\theta_1,\theta_2)$ can be written as [10]

$$\sigma_{\rm cap}(E_{\rm c.m.},\theta_1,\theta_2) = \frac{\pi\hbar^2}{2\mu E_{\rm c.m.}}\sum_J (2J+1)T(E_{\rm c.m.},\theta_1,\theta_2,J). \tag{3}$$

Here, the transmission probability is given by

$$T(E_{\rm c.m.},\theta_1,\theta_2,J) = \frac{1}{1+\exp\left\{-\frac{2\pi}{\hbar\omega(\theta_1,\theta_2,J)}\left[E_{\rm c.m.}-B(\theta_1,\theta_2)-\frac{\hbar^2}{2\mu R_{\rm B}^2(\theta_1,\theta_2,J)}\right]\right\}}, \tag{4}$$

where $\hbar\omega(\theta_1,\theta_2,J)$ is the width of the parabolic barrier, and $R_{\rm B}(\theta_1,\theta_2,J)$ defines a position of the barrier.

The nucleus-nucleus interaction potential with quadrupole deformation in the calculation is taken as the form

$$V(r,\theta_1,\theta_2) = V_{\rm N}(r,\theta_1,\theta_2) + V_{\rm C}(r,\theta_1,\theta_2). \tag{5}$$

The nuclear potential and Coulomb potential are taken as the forms in Ref. [27], i.e.,

$$V_{\rm N}(r,\theta_1,\theta_2) = -V_0\left\{1+\exp\left[\left(r-\sum_{i=1}^{2}R_i\left[1+(5/4\pi)^{1/2}\beta_2^{(i)}P_2(\cos\theta_i)\right]\right)a^{-1}\right]\right\}^{-1}, \tag{6}$$

and

$$V_{\rm C}(r,\theta_1,\theta_2) = \frac{Z_1Z_2e^2}{r} + \left(\frac{9}{20\pi}\right)^{1/2}\left(\frac{Z_1Z_2e^2}{r^3}\right)\sum_{i=1}^{2}R_i^2\beta_2^{(i)}P_2(\cos\theta_i) + \left(\frac{3}{7\pi}\right)\left(\frac{Z_1Z_2e^2}{r^3}\right)\sum_{i=1}^{2}R_i^2\left[\beta_2^{(i)}P_2(\cos\theta_i)\right]^2, \tag{7}$$

where θ_i is the angle between the symmetry axis of the ith nucleus and the collision axis as shown in Fig. 1. $\beta_2^{(i)}$ and R_i are the quadrupole deformation parameter and the radius of the ith nucleus, respectively. The strength V_0 and diffusion width a of the nuclear potential are set to be 80.0 MeV and 0.70 fm in this work, respectively. The quadrupole deformation parameter is taken from Ref. [28]. Comparing with the empirical coupled-channel model introduced in Refs. [10,29], almost no adjustable parameter is required in this method. The capture cross section for Ca-induced hot fusion reactions can be written as

$$\sigma_{\rm cap}(E_{\rm c.m.}) = \frac{1}{2}\int_0^{\pi}\sigma_{\rm cap}(E_{\rm c.m.},\theta_2)\sin\theta_2\,d\theta_2, \tag{8}$$

where the orientation effects of only the deformed targets are considered.

In this work, we concentrate on the phenomenological relationship between physical quantities and $P_{\rm CN}$. According to the dinuclear system (DNS) concept, the fusion probability strongly depends on the mass asymmetry $\eta = (A_{\rm T}-A_{\rm P})/(A_{\rm T}+A_{\rm P})$. The inner fusion barrier increases with reducing mass asymmetry, which leads to a decrease of the formation probability of the compound nucleus. The influence of entrance channel mass asymmetry η and excitation energy of the compound nucleus E^* on fusion probability are relatively clear in the DNS model [12,30]. The size of the potential pocket also could influence fusion probability. Figure 2(a) shows the entrance channel potential for the reaction ^{48}Ca + ^{238}U. The minimum value of the potential pocket at $R_{\rm m}$ and $R_{\rm B}$ denotes the barrier position. The depth of the potential pocket $B_{\rm qf}$ is also shown. The solid point on the potential curve denotes the position when two colliding nuclei come into contact. The nucleon transfer process usually takes place at the minimum position of the interaction potential after capture of the colliding system. In the DNS concept, the size of the potential pocket, which is determined by quasifission barrier $B_{\rm qf}$ and ΔR, strongly influences the decay time of the DNS [31] and fusion probability. The influence of $B_{\rm qf}$ on fusion probability has been discussed in many works [19,31–33]. Usually, a deeper potential pocket corresponds to a wider ΔR. The larger distance ΔR can cause more kinetic energy dissipating at the quasifission process, which could lower the quasifission probability. Therefore, in this work we only concern the value of ΔR to describe the size of the potential pocket. The nucleon collectivization mechanism proposed in Ref. [10] has a similar opinion that a larger potential pocket probably results in a higher fusion probability. It is assumed that when two colliding nuclei touch each other the number of collectivized nucleons starts increasing until all nucleons are collectivized and the compound nucleus is formed. If the capture pocket is large, many quasibound states exist. Then the coupling to complex states is strong and the probability of compound nucleus formation is much larger than for small pockets [34]. Therefore, it is reasonable to

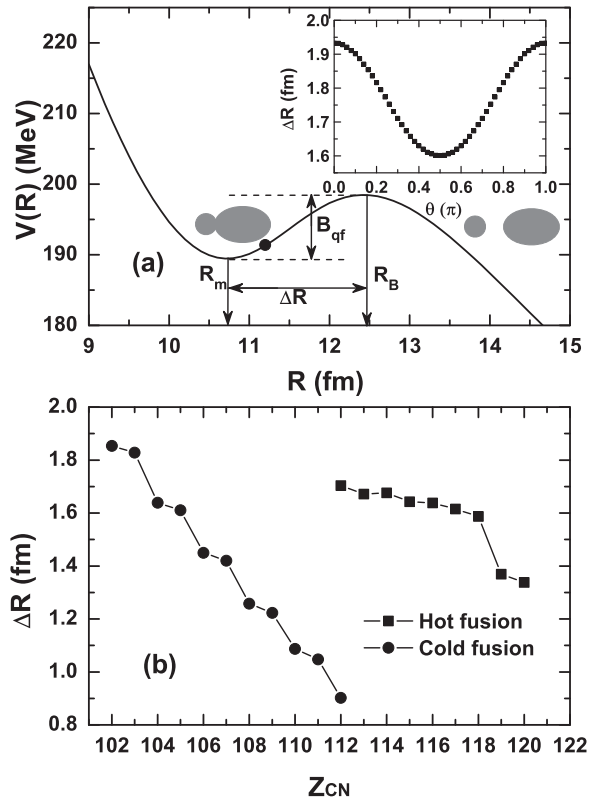

FIG. 2. (a) Nucleus-nucleus interaction potential of the reaction ^{48}Ca + ^{238}U. The solid circle on the curve denotes the position where two colliding nuclei touch. The inset is the orientation dependence of ΔR. (b) ΔR as a function of charge number of compound nucleus Z_{CN}. The solid circles and solid squares denote cold and hot fusion reactions, respectively. The ^{50}Ti induced reactions for synthesizing SHEs $Z = 119$ and 120 are also shown.

conclude that a larger potential pocket probably results in a higher fusion probability. The orientation effects are also quite important for calculating the fusion probability. Orientation effects of the fusion probability were investigated in reactions with deformed nuclei [35–37]. The experimental results show that the fusion probability is higher at equatorial orientation ($\theta_{1,2} = \pi/2$) because of the more compact configuration.

The inset of Fig. 2(a) shows the orientation effects of ΔR for the reaction ^{48}Ca + ^{238}U. One can see that ΔR strongly depends on the orientation of the target. ΔR of polar orientation of ^{238}U ($\theta_2 = 0$) is larger than that of the equatorial orientation ($\theta_2 = \pi/2$). Figure 2(b) shows ΔR as a function of charge number of compound nucleus Z_{CN}. One can see ΔR decreases with the increasing Z_{CN} for both cold and hot fusion reactions. The ΔR is very small for synthesizing elements $Z \geqslant 112$ in cold fusion reactions while the hot fusion reactions give larger value of ΔR. Therefore, it is very hard to synthesize the SHEs $Z \geqslant 112$ in cold fusion reactions.

One can find the exponential increase of P_{CN} with increasing $E_{c.m.}$ and η in Refs. [12,30,38]. Therefore, we assume fusion probability increases exponentially as $1/\eta$, ΔR, and excitation energy of the compound nucleus E^* increase. We also assume P_{CN} is independent of angular momentum as reported in Ref. [18]. Considering the contributions of the potential pocket, E^*, and the orientation effects, we propose an analytical formula to describe the fusion probability P_{CN},

$$P_{CN}(E^*,\theta_1,\theta_2) = \exp\left(\frac{C_0}{\eta}\right)\exp[C_1\Delta R(\theta_1,\theta_2)] \times \exp\left(C_2\frac{R(\theta_2)-R_{side}}{R_{tip}-R_{side}}\right)\exp(C_3E^*), \quad (9)$$

where $\Delta R = R_B - R_m$ as shown in Fig. 2. The constants C_0, C_1, and C_3 equal -10.8, 7 fm^{-1}, and 0.01 MeV^{-1}, respectively. The third term describes the orientation effects of the fusion probability. $C_2(=aA_{CN}^{1/3}+b)$ depends on the size of the colliding system, which is considered as a hindrance of fusion at the polar orientation of the deformed target, where $a = -78$ and $b = 508.5$. The constants in Eq. (9) are determined just by fitting the experimental ER cross sections of the hot reactions ^{48}Ca + ^{238}U, ^{48}Ca + ^{242}Pu, and ^{48}Ca + ^{244}Pu and the cold fusion reaction ^{48}Ca + ^{208}Pb. The parameters a and b are obtained by linear fitting of C_2 for the hot reactions ^{48}Ca + ^{238}U, ^{48}Ca + ^{242}Pu, and ^{48}Ca + ^{244}Pu. R_{tip} and R_{side} are the semimajor axis and semiminor axis of the prolate deformed target as shown in Fig. 1. $E^* = E_{c.m.} + Q$, where $Q = M(P)c^2 + M(T)c^2 - M(C)c^2$; and $M(P)$, $M(T)$, and $M(C)$ are the nuclear masses of projectile, target, and compound nucleus, respectively. In this work, the mass table of Möller [39] is used. Because of the spherical nuclei in the cold fusion reactions, the capture cross section cannot be calculated using the method that we proposed in this work. Therefore, the method in Ref. [29] is used. Since the colliding nuclei in cold fusion reactions are almost spherical, the fusion probability is calculated without considering the orientation effects. Then Eq. (9) becomes $P_{CN}(E^*) = \exp(\frac{C_0}{\eta})\exp(C_1\Delta R)\exp(C_3E^*)$. In this work, the fusion cross section is defined by the product of the capture cross section and the fusion probability P_{CN}:

$$\sigma_{fus}(E_{c.m.}) = \frac{1}{4}\int_0^\pi \sin\theta_1 d\theta_1 \int_0^\pi \sigma_{cap}(E_{c.m.},\theta_1,\theta_2) \times P_{CN}(E_{c.m.},\theta_1,\theta_2)\sin\theta_2\, d\theta_2. \quad (10)$$

III. RESULTS AND DISCUSSION

In this section the approach described above is applied to analyze the available experimental data on the synthesis of SHN. The parameters of Eq. (9) keep the same values for all reactions. The production cross sections of SHEs with $Z = 119$ and 120 are analyzed.

A. Comparisons with experimental data and other models

In Fig. 3 the experimental ER cross sections for the cold fusion reactions ^{48}Ca + ^{208}Pb [40], ^{70}Zn + ^{208}Pb [1], and ^{70}Zn + ^{209}Bi [8] are compared with the calculated results in this work. One can see that the calculated results of ER cross sections are in good agreement with available experimental data. For these reactions the capture cross sections are calculated by using the method in Ref. [29].

As an example of calculating capture cross section in this work, Fig. 4(a) shows the comparison of capture cross section

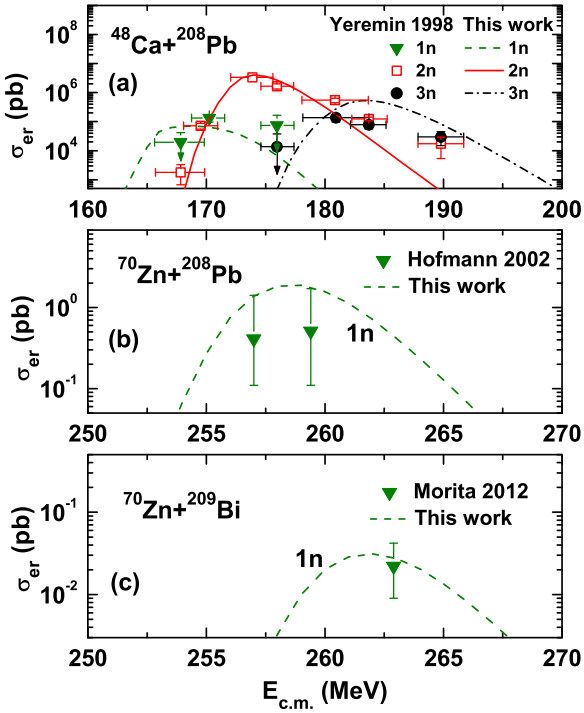

FIG. 3. (Color online) Comparison of the calculated ER cross sections and the experimental data for the cold fusion reactions ^{48}Ca + ^{208}Pb (Yeremin 1998 [40]) (a), ^{70}Zn + ^{208}Pb (Hofmann 2002 [1]) (b), and ^{70}Zn + ^{209}Bi (Morita 2012 [8]) (c) for synthesis of superheavy elements $Z = 102$, 112, and 113, respectively. The experimental data of ER cross sections of the $1n$, $2n$, and $3n$ channels are denoted by solid triangles, squares, and circles, respectively. The calculated results are denoted by lines.

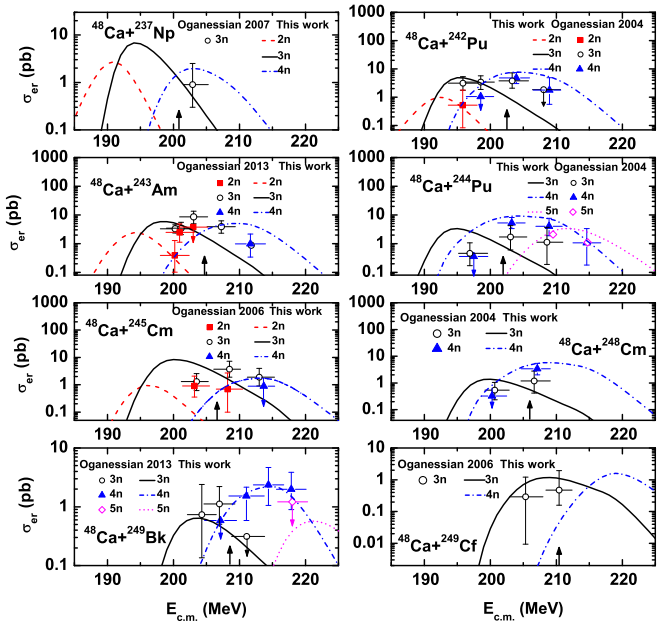

FIG. 5. (Color online) Comparison of the calculated ER cross sections with the available experimental data for the reactions ^{48}Ca + ^{237}Np (Oganessian 2007 [6]), ^{242}Pu (Oganessian 2004 [5]), ^{243}Am (Oganessian 2013 [3]), ^{244}Pu (Oganessian 2004 [2]), ^{245}Cm (Oganessian 2006 [4]), ^{248}Cm (Oganessian 2004 [5]), ^{249}Bk (Oganessian 2013 [7]), and ^{249}Cf (Oganessian 2006 [4]). The measured ER cross sections of the $2n$, $3n$, $4n$, and $5n$ channels are denoted by solid squares, circles, triangles, and diamonds, respectively. The calculated results in this work are denoted by lines. The arrows show positions of the corresponding Coulomb barriers.

results in this work with the experimental data [41] for the ^{48}Ca + ^{238}U fusion reaction. The calculated results are in good agreement with the experimental data. Figure 4(b) shows the

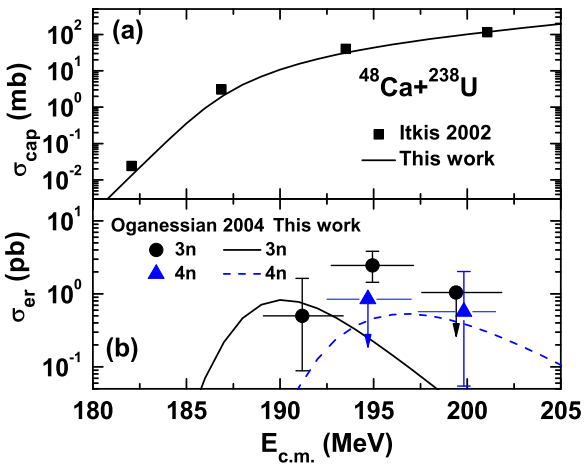

FIG. 4. (Color online) (a) Capture cross sections for the ^{48}Ca + ^{238}U fusion reaction. The experimental data (Itkis 2002 [41]) are denoted by solid squares. (b) ER cross sections for the ^{48}Ca + ^{238}U fusion reaction. The experimental data of ER cross sections (Oganessian 2004 [5]) of the $3n$ and $4n$ channels are denoted by solid circles and solid triangles, respectively.

ER cross sections. Within the error bars, the experimental data [5] are reproduced rather well, especially for the $4n$ channel.

To test the method, the ER cross sections for the reactions ^{48}Ca + ^{237}Np, ^{242}Pu, ^{243}Am, ^{244}Pu, ^{245}Cm, ^{248}Cm, ^{249}Bk, and ^{249}Cf to produce elements $Z = 113$–118 are shown in Fig. 5. The same parameters of Eq. (9), which are determined just by the reactions ^{48}Ca + ^{238}U, ^{48}Ca + ^{242}Pu, ^{48}Ca + ^{244}Pu, and ^{48}Ca + ^{208}Pb, are used. The experimental data [2–7] are reproduced rather well for all reactions. We predict the maximal ER cross section of the reaction ^{48}Ca + ^{249}Cf for the $4n$ channel to be 1.58 pb and the corresponding optimal incident energy is $E_{\rm c.m.} = 219$ MeV. The arrows show positions of the corresponding Coulomb barriers. For most of the hot fusion reactions, the position of the Coulomb barrier is close to that of the optimal incident energy, which corresponds to the maximal ER cross section of the $4n$ channel. The same phenomenon is also shown in Ref. [19].

To further test Eq. (9), Fig. 6 compares the values of $P_{\rm CN}$ calculated in this work with predictions in Refs. [9,12,42–44] for the synthesis of $Z = 102$–113 in cold fusion reactions. The experimental data [45] for the reaction ^{50}Ti + ^{208}Pb is also shown. The calculations are for an excitation energy of 15 MeV. The same parameters of Eq. (9) are used. The orientation effects are not considered because of spherical targets in cold fusion reactions. The fusion probability decreases rapidly with the increasing $Z_{\rm CN}$. The curve of this work locates in the

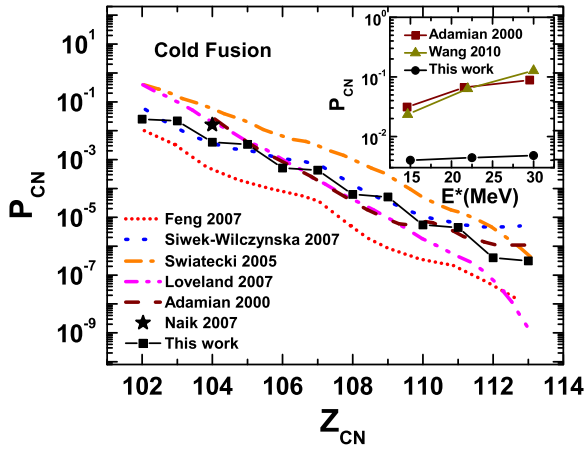

FIG. 6. (Color online) Comparison of predictions of P_{CN} calculated in this work with the data from Feng 2007 [12], Siwek-Wilczynska 2007 [42], Swiatecki 2005 [43], Loveland 2007 [44], Adamian 2000 [9], and Naik 2007 [45] for synthesis of elements $Z = 102$–113 in cold fusion reactions based on ^{208}Pb and ^{209}Bi targets with projectile nuclei ^{48}Ca, ^{50}Ti, ^{54}Cr, ^{58}Fe, ^{64}Ni, and ^{70}Zn. The inset is predictions of P_{CN} as a function of excitation energy E^* for the system ^{50}Ti + ^{208}Pb calculated in this work and results from Adamian 2000 [9] and Wang 2010 [46].

middle of other predictions and the trend of the curve is close to others. The inset shows the P_{CN} as a function of excitation energy E^* for the reaction ^{50}Ti + ^{208}Pb. One can see that P_{CN} increases exponentially with increasing E^*. The behavior is close to the results from Refs. [9,46].

Figure 7 shows the orientation effects of fusion probability for the reaction ^{48}Ca + ^{238}U at $E^* = 40$ MeV. The fusion probability that corresponds to the equatorial orientation of the ^{238}U nucleus ($\theta_2 = \pi/2$) is much larger. The results from the DNS model with angular momentum $J = 0$ are also shown. A similar behavior can be seen. Therefore, the orientation effects of Eq. (9) are reasonable.

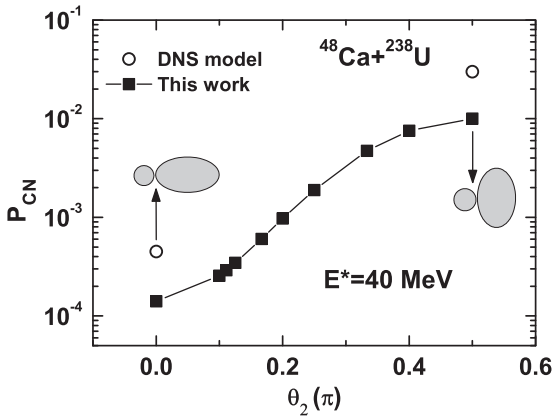

FIG. 7. Fusion probability as a function of orientation angle θ_2 for the reaction ^{48}Ca + ^{238}U at $E^* = 40$ MeV. The circles denote the results from the DNS model.

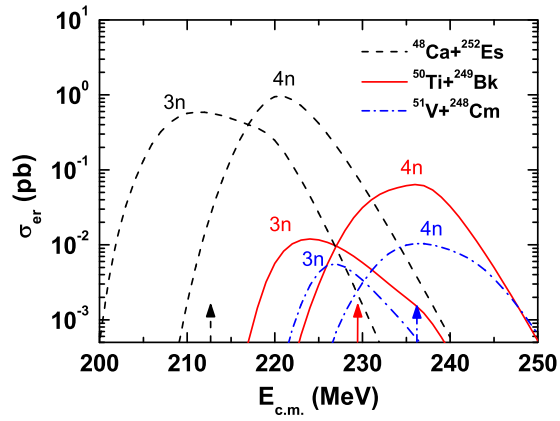

FIG. 8. (Color online) ER cross sections as a function of the incident energy for the reactions ^{48}Ca + ^{252}Es (dashed lines), ^{50}Ti + ^{249}Bk (solid lines), and ^{51}V + ^{248}Cm (dot-dashed lines) for producing element $Z = 119$. The dashed, solid, and dot-dashed arrows show positions of the Coulomb barriers for the respective reactions.

B. Evaporation residue cross sections of $Z = 119$ and 120

The above calculations give us confidence in our method to investigate the ER cross sections of fusion reactions leading to new elements. The ER cross sections of the reactions ^{48}Ca + ^{252}Es, ^{50}Ti + ^{249}Bk, and ^{51}V + ^{248}Cm for producing the superheavy element $Z = 119$ are shown in Fig. 8. The dashed, solid, and dot-dashed arrows denote the positions of the entrance channel Coulomb barriers for the reactions ^{48}Ca + ^{252}Es, ^{50}Ti + ^{249}Bk, and ^{51}V + ^{248}Cm, respectively. The maximal ER cross sections of the $3n$ and $4n$ channels in the reaction ^{48}Ca + ^{252}Es are 0.59 and 0.96 pb for the incident energies $E_{c.m.} = 211$ and 221 MeV, respectively. The ER cross sections from Ref. [32] within the framework of a dinuclear system model are in the same order of magnitude, while the maximal cross section of the $3n$ channel, which is 0.3 pb, is larger than that of the $4n$ channel. The maximal cross section for the reaction ^{50}Ti + ^{249}Bk is 0.064 pb in the $4n$ emission channel and the optimal incident energy is $E_{c.m.} = 236$ MeV, which is close to the results from Ref. [17], where the maximal cross section and optimal incident energy is about 0.050 pb and $E_{c.m.} = 236$ MeV, respectively. It can be seen that the maximal ER cross section for the reaction ^{51}V + ^{248}Cm is only 0.01 pb in the $4n$ channel and the corresponding incident energy is $E_{c.m.} = 237$ MeV. The reason for larger ER cross sections of the reaction ^{48}Ca + ^{252}Es probably is that the fusion probability increases considerably as the mass asymmetry increases. This is connected with the strong hindrance to formation of compound nucleus due to the dominant role of the quasifission process. Therefore, the reaction ^{48}Ca + ^{252}Es would be better for synthesizing the superheavy element $Z = 119$ if enough of the ^{252}Es can be collected to make a target.

Figure 9 shows the ER cross sections of the reactions ^{50}Ti + ^{249}Cf, ^{54}Cr + ^{248}Cm, and ^{51}V + ^{249}Bk for producing the superheavy element $Z = 120$. The arrows denote the positions of the entrance channel Coulomb barriers for each reaction. The ER cross sections of 3n and $4n$ channels for the reaction ^{50}Ti + ^{249}Cf are obviously greater than those of systems ^{54}Cr + ^{248}Cm and ^{51}V + ^{249}Bk. The reason probably is

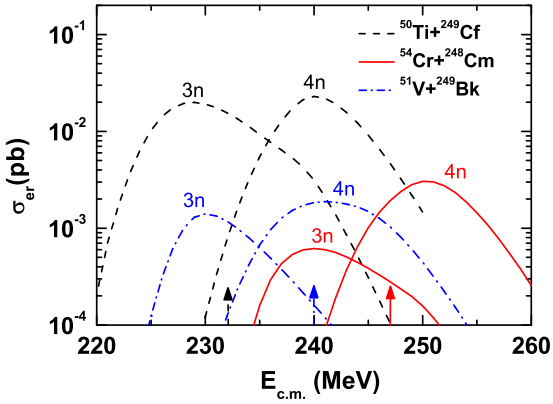

FIG. 9. (Color online) ER cross sections as a function of the incident energy for the reactions ^{50}Ti + ^{249}Cf (dashed lines), ^{54}Cr + ^{248}Cm (solid lines), and ^{51}V + ^{249}Bk (dot-dashed lines) for producing element $Z = 120$. The dashed, solid, and dot-dashed arrows show positions of the Coulomb barriers for the respective reactions.

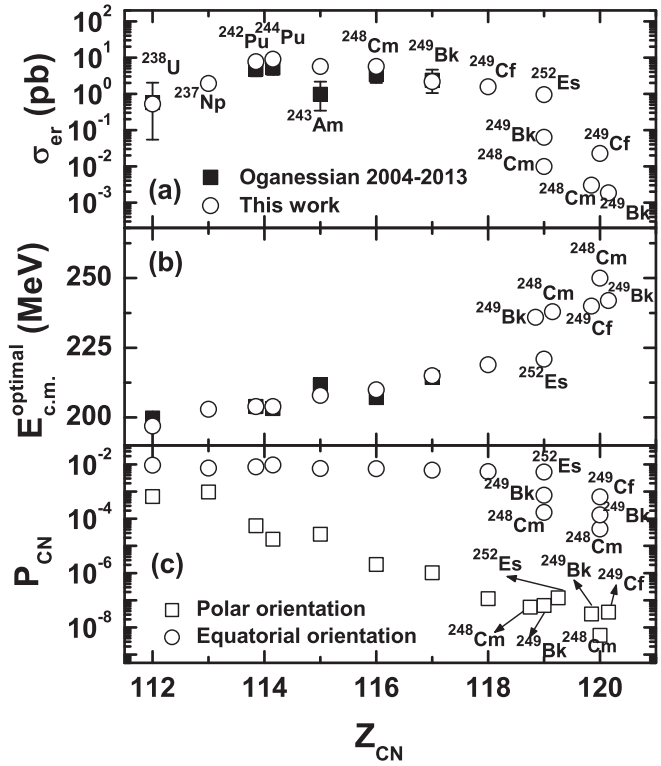

FIG. 10. Maximal values of experimental available ER cross sections (Oganessian 2007 [6], Oganessian 2004 [5], Oganessian 2013 [3], Oganessian 2004 [2], Oganessian 2006 [4], Oganessian 2004 [5], Oganessian 2013 [7], and Oganessian 2006 [4]) of the 4n channel (a) and corresponding optimal incident energies (b) for hot fusion reactions to produce elements $Z = 112$–118, in comparison with the theoretical values calculated in this work. The maximal ER cross sections and optimal incident energies for $Z = 119$ and 120 are also predicted. (c) The calculated fusion probabilities of hot fusion reactions as a function of Z_{CN} for equatorial and polar orientations. The reactions are denoted by actinide targets.

that the fusion probability of the system ^{50}Ti + ^{249}Cf is larger due to more mass asymmetry of the entrance channel. The production cross sections for the reactions ^{54}Cr + ^{248}Cm and ^{51}V + ^{249}Bk are 0.003 and 0.0018 pb, respectively, which are too small for available facilities. The predicted maximal ER cross section and optimal bombarding energy of the reaction ^{50}Ti + ^{249}Cf are 0.029 pb and $E_{c.m.} = 240$ MeV, respectively, which are close to the results from Ref. [17]. The maximal ER cross section of the reaction ^{50}Ti + ^{249}Cf is quite reachable at available setups, though a longer time of irradiation is needed.

In this work, the calculated maximal ER cross sections of producing SHEs with $Z = 119$ and 120 are in the 4n channel. In Fig. 10(a), the maximal ER cross sections of the 4n channel in hot fusion reactions to produce elements $Z = 112$–118 are compared with the the available experimental data. Figure 10(b) shows the corresponding optimal incident energies. One can see the calculated results of maximal ER cross sections of the 4n channel and corresponding incident energies are in good agreement with the available experimental data. The maximal ER cross section of the 4n channel of the reaction ^{48}Ca + ^{237}Np for producing $Z = 113$ is 1.96 pb and the corresponding incident energy is $E_{c.m.} = 203$ MeV. The calculated maximal ER cross sections and corresponding incident energies for the reactions ^{48}Ca + ^{252}Es$\rightarrow^{(300-4n)}$119, ^{50}Ti + ^{249}Bk$\rightarrow^{(299-4n)}$119, ^{51}V + ^{248}Cm$\rightarrow^{(299-4n)}$119, ^{50}Ti + ^{249}Cf$\rightarrow^{(299-4n)}$120, ^{54}Cr + ^{248}Cm$\rightarrow^{(302-4n)}$120, and ^{51}V + ^{249}Bk$\rightarrow^{(300-4n)}$120 are also shown. One behavior that can be seen is that the system has larger maximal ER cross section of the 4n channel corresponding to lower optimal incident energy. The reason is probably that the survival probability is larger for a reaction with lower optimal incident energy, which is connected with the lower excitation energy of the compound nucleus. The optimal incident energy of the 4n channel is probably related to the Coulomb barrier height. Figure 10(c) shows the calculated fusion probabilities of hot fusion reactions as a function of Z_{CN} for polar and equatorial configurations. The fusion probability of each system is calculated at optimal incident energies which are shown in Fig. 10(b). One can see that the fusion probabilities for polar orientation decrease rapidly with increasing charge number of the synthesized compound nucleus, while the trend is almost flat for equatorial orientation. The reason probably is that the size of the potential pocket for polar orientation is more sensitive to Z_{CN}.

IV. CONCLUSIONS

In summary, in hot fusion reactions with deformed targets, only the deformation effect is considered for barrier distribution and almost no adjustable parameter is required to calculate capture cross section. An empirical formula is proposed to calculate the fusion probability of both cold and hot fusion reactions. In the formula, the orientation effect is considered. The calculated ER cross sections of hot fusion reactions show a good agreement with the experimental data. The formula also can give reasonable results of fusion probabilities in cold fusion reactions. The production cross sections of $Z = 119$ and 120 are predicted. The maximal ER cross sections of the reactions ^{48}Ca + ^{252}Es, ^{50}Ti + ^{249}Bk, and

$^{51}V + ^{248}Cm$ for synthesizing element 119 are 0.96, 0.064, and 0.01 pb in the $4n$ emission channel for the optimal incident energies $E_{c.m.} = 221$, 236, and 237 MeV, respectively. In the projectile-target combinations $^{50}Ti + ^{249}Cf$, $^{54}Cr + ^{248}Cm$, and $^{51}V + ^{249}Bk$ leading to synthesis of SHN with $Z = 120$, the maximal ER cross sections are 0.029, 0.003 and 0.0018 pb in $4n$ emission channel for the optimal incident energies $E_{c.m.} = 240$, 250, and 242 MeV, respectively. It is found that for hot fusion reactions larger maximal ER cross section of the $4n$ channel corresponds to lower optimal incident energy. In hot fusion reactions, the fusion probabilities for polar orientation decrease rapidly with increasing charge number of the synthesized compound nucleus, while the trend is almost flat for equatorial orientation.

ACKNOWLEDGMENTS

This work was supported by the National Natural Science Foundation of China under Grants No. 11025524 and No. 11161130520, National Basic Research Program of China under Grant No. 2010CB832903, and the European Commission's 7th Framework Programme (FP7-PEOPLE-2010-IRSES) under Grant Agreement Project No. 269131.

[1] S. Hofmann and G. Münzenberg, Rev. Mod. Phys. **72**, 733 (2000); S. Hofmann, F. P. Heßberger, D. Ackermann, G. Münzenberg, S. Antalic, P. Cagarda, B. Kindler, J. Kojouharova, M. Leino, B. Lommel, R. Mann, A. G. Popeko, S. Reshitko, S. Śaro, J. Uusitalo, and A. V. Yeremin, Eur. Phys. J. A **14**, 147 (2002).

[2] Y. T. Oganessian, V. K. Utyonkov, Y. V. Lobanov, F. S. Abdullin, A. N. Polyakov, I. V. Shirokovsky, Y. S. Tsyganov, G. G. Gulbekian, S. L. Bogomolov, B. N. Gikal, A. N. Mezentsev, S. Iliev, V. G. Subbotin, A. M. Sukhov, A. A. Voinov, G. V. Buklanov, K. Subotic, V. I. Zagrebaev, M. G. Itkis, J. B. Patin, K. J. Moody, J. F. Wild, M. A. Stoyer, N. J. Stoyer, D. A. Shaughnessy, J. M. Kenneally, P. A. Wilk, R. W. Lougheed, R. I. Ilkaev, and S. P. Vesnovskii, Phys. Rev. C **69**, 054607 (2004).

[3] Yu. Ts. Oganessian, F. Sh. Abdullin, S. N. Dmitriev, J. M. Gostic, J. H. Hamilton, R. A. Henderson, M. G. Itkis, K. J. Moody, A. N. Polyakov, A. V. Ramayya, J. B. Roberto, K. P. Rykaczewski, R. N. Sagaidak, D. A. Shaughnessy, I. V. Shirokovsky, M. A. Stoyer, N. J. Stoyer, V. G. Subbotin, A. M. Sukhov, Yu. S. Tsyganov, V. K. Utyonkov, A. A. Voinov, and G. K. Vostokin, Phys. Rev. C **87**, 014302 (2013).

[4] Yu. Ts. Oganessian, V. K. Utyonkov, Yu. V. Lobanov, F. Sh. Abdullin, A. N. Polyakov, R. N. Sagaidak, I. V. Shirokovsky, Yu. S. Tsyganov, A. A. Voinov, G. G. Gulbekian, S. L. Bogomolov, B. N. Gikal, A. N. Mezentsev, S. Iliev, V. G. Subbotin, A. M. Sukhov, K. Subotic, V. I. Zagrebaev, G. K. Vostokin, M. G. Itkis, K. J. Moody, J. B. Patin, D. A. Shaughnessy, M. A. Stoyer, N. J. Stoyer, P. A. Wilk, J. M. Kenneally, J. H. Landrum, J. F. Wild, and R. W. Lougheed, Phys. Rev. C **74**, 044602 (2006).

[5] Yu. Ts. Oganessian, V. K. Utyonkov, Yu. V. Lobanov, F. Sh. Abdullin, A. N. Polyakov, I. V. Shirokovsky, Yu. S. Tsyganov, G. G. Gulbekian, S. L. Bogomolov, B. N. Gikal, A. N. Mezentsev, S. Iliev, V. G. Subbotin, A. M. Sukhov, A. A. Voinov, G. V. Buklanov, K. Subotic, V. I. Zagrebaev, M. G. Itkis, J. B. Patin, K. J. Moody, J. F. Wild, M. A. Stoyer, N. J. Stoyer, D. A. Shaughnessy, J. M. Kenneally, P. A. Wilk, R. W. Lougheed, R. I. Il'kaev, and S. P. Vesnovskii, Phys. Rev. C **70**, 064609 (2004).

[6] Yu. Ts. Oganessian, V. K. Utyonkov, Yu. V. Lobanov, F. Sh. Abdullin, A. N. Polyakov, R. N. Sagaidak, I. V. Shirokovsky, Yu. S. Tsyganov, A. A. Voinov, G. G. Gulbekian, S. L. Bogomolov, B. N. Gikal, A. N. Mezentsev, V. G. Subbotin, A. M. Sukhov, K. Subotic, V. I. Zagrebaev, G. K. Vostokin, M. G. Itkis, R. A. Henderson, J. M. Kenneally, J. H. Landrum, K. J. Moody, D. A. Shaughnessy, M. A. Stoyer, N. J. Stoyer, and P. A. Wilk, Phys. Rev. C **76**, 011601(R) (2007).

[7] Yu. Ts. Oganessian, F. Sh. Abdullin, C. Alexander, J. Binder, R. A. Boll, S. N. Dmitriev, J. Ezold, K. Felker, J. M. Gostic, R. K. Grzywacz, J. H. Hamilton, R. A. Henderson, M. G. Itkis, K. Miernik, D. Miller, K. J. Moody, A. N. Polyakov, A. V. Ramayya, J. B. Roberto, M. A. Ryabinin, K. P. Rykaczewski, R. N. Sagaidak, D. A. Shaughnessy, I. V. Shirokovsky, M. V. Shumeiko, M. A. Stoyer, N. J. Stoyer, V. G. Subbotin, A. M. Sukhov, Yu. S. Tsyganov, V. K. Utyonkov, A. A. Voinov, and G. K. Vostokin, Phys. Rev. C **87**, 054621 (2013).

[8] K. Morita, K. Morimoto, D. Kaji, H. Haba, K. Ozeki, Y. Kudou, T. Sumita, Y. Wakabayashi, A. Yoneda, K. Tanaka, S. Yamaki, R. Sakai, T. Akiyama, S. Goto, H. Hasebe, M. Huang, T. Huang, E. Ideguchi, Y. Kasamatsu, K. Katori, Y. Kariya, H. Kikunaga, H. Koura, H. Kudo, A. Mashiko, K. Mayama, S. Mitsuoka, T. Moriya, M. Murakami, H. Murayama, S. Namai, A. Ozawa, N. Sato, K. Sueki, M. Takeyama, F. Tokanai, T. Yamaguchi, and A. Yoshida, J. Phys. Soc. Jpn. **81**, 103201 (2012).

[9] G. G. Adamian, N. V. Antonenko, and W. Scheid, Nucl. Phys. A **678**, 24 (2000).

[10] V. I. Zagrebaev, Phys. Rev. C **64**, 034606 (2001).

[11] Z. H. Liu and J. D. Bao, Phys. Rev. C **87**, 034616 (2013).

[12] Z. Q. Feng, G. M. Jin, J. Q. Li, and W. Scheid, Phys. Rev. C **76**, 044606 (2007).

[13] K. Siwek-Wilczyńska, T. Cap, M. Kowal, A. Sobiczewski, and J. Wilczyński, Phys. Rev. C **86**, 014611 (2012).

[14] N. Wang, E. G. Zhao, W. Scheid, and S. G. Zhou, Phys. Rev. C **85**, 041601(R) (2012).

[15] C. W. Shen, Y. Abe, D. Boilley, G. Kosenko, and E. G. Zhao, Int. J. Mod. Phys. E **17**, 66 (2008).

[16] G. Mandaglio, G. Giardina, A. K. Nasirov, and A. Sobiczewski, Phys. Rev. C **86**, 064607 (2012).

[17] V. Zagrebaev and W. Greiner, Phys. Rev. C **78**, 034610 (2008).

[18] R. Smolańczuk, Phys. Rev. C **81**, 067602 (2010).

[19] N. Wang, J. Tian, and W. Scheid, Phys. Rev. C **84**, 061601(R) (2011).

[20] K. Sandhu, M. K. Sharma, and R. K. Gupta, Phys. Rev. C **85**, 024604 (2012).

[21] V. I. Zagrebaev, A. V. Karpov, and W. Greiner, Phys. Rev. C **85**, 014608 (2012).

[22] A. K. Nasirov, G. Mandaglio, G. Giardina, A. Sobiczewski, and A. I. Muminov, Phys. Rev. C **84**, 044612 (2011).

[23] W. Reisdorf, Z. Phys. A **300**, 227 (1981).
[24] W. Reisdorf and M. Schädel, Z. Phys. A **343**, 47 (1992).
[25] J. R. Leigh, M. Dasgupta, D. J. Hinde, J. C. Mein, C. R. Morton, R. C. Lemmon, J. P. Lestone, J. O. Newton, H. Timmers, J. X. Wei, and N. Rowley, Phys. Rev. C **52**, 3151 (1995).
[26] L. Zhu, J. Su, W. J. Xie, and F. S. Zhang, Nucl. Phys. A **915**, 90 (2013).
[27] C. Y. Wong, Phys. Rev. Lett. **31**, 766 (1973).
[28] S. GORIELY, F. TONDEUR, and J. M. PEARSON, At. Data Nucl. Data Tables **77**, 311 (2001).
[29] Z. Q. Feng, G. M. Jin, F. Fu, and J. Q. Li, Nucl. Phys. A **771**, 50 (2006).
[30] G. G. Adamian, N. V. Antonenko, and W. Scheid, J. Phys.: Conf. Ser. **322**, 012009 (2011).
[31] A. K. Nasirov, G. Giardina, G. Mandaglio, M. Manganaro, and W. Scheid, J. Phys.: Conf. Ser. **282**, 012010 (2011).
[32] M. H. Huang, Z. G. Gan, X. H. Zhou, J. Q. Li, and W. Scheid, Phys. Rev. C **82**, 044614 (2010).
[33] G. Giardina, S. Hofmann, A. I. Muminov, and A. K. Nasirov, Eur. Phys. J. A **8**, 205 (2000).
[34] V. Yu. Denisov and W. Nörenberg, Eur. Phys. J. A **15**, 375 (2002).
[35] K. Nishio, H. Ikezoe, S. Mitsuoka, I. Nishinaka, Y. Nagame, Y. Watanabe, T. Ohtsuki, K. Hirose, and S. Hofmann, Phys. Rev. C **77**, 064607 (2008).
[36] K. Nishio, H. Ikezoe, S. Mitsuoka, and J. Lu, Phys. Rev. C **62**, 014602 (2000).
[37] Yu. Ts. Oganessian, J. Phys. G **34**, R165 (2007).
[38] K. Nishio, S. Mitsuoka, I. Nishinaka, H. Makii, Y. Wakabayashi, H. Ikezoe, K. Hirose, T. Ohtsuki, Y. Aritomo, and S. Hofmann, Phys. Rev. C **86**, 034608 (2012).
[39] P. Möller and J. R. Nix, J. Phys. G: Nucl. Part. Phys. **20**, 1681 (1994).
[40] A. V. Yeremin, V. I. Chepigin, M. G. Itkis, A. P. Kabachenko, S. P. Korotkov, O. N. Malyshev, Yu. Ts. Oganessian, A. G. Popeko, J. Rohac, R. N. Sagaidak, M. L. Chelnokov, V. A. Gorshkov, A. Yu. Lavrentev, S. Hofmann, G. Münzenberg, Š. Šáro, K. Morita, N. Iwasa, S. I. Mulgin, and S. V. Zhdanov, JINR Rapid Commun. **92**, 21 (1998).
[41] M. G. Itkis, A. A. Bogatchev, I. M. Itkis, M. Jandel, J. Kliman, G. N. Kniajeva, N. A. Kondratiev, I. V. Korzyukov, E. M. Kozulin, L. Krupa, Yu. Ts. Oganessian, I. V. Pokrovski, V. A. Ponomarenko, E. V. Prokhorova, A. Ya. Rusanov, V. M. Voskresenski, A. A. Goverdovski, F. Hanappe, T. Materna, N. Rowley, L. Stuttge, G. Giardina, and K. J. Moody, J. Nucl. Radiochem. Sci. **3**, 57 (2002).
[42] K. Siwek-Wilczynska, I. Skwira-Chalot, and J. Wilczynski, Int. J. Mod. Phys. E **16**, 483 (2007).
[43] W. J. Swiatecki, K. Siwek-Wilczynska, and J. Wilczynski, Phys. Rev. C **71**, 014602 (2005).
[44] W. Loveland, Phys. Rev. C **76**, 014612 (2007).
[45] R. S. Naik, W. Loveland, P. H. Sprunger, A. M. Vinodkumar, D. Peterson, C. L. Jiang, S. Zhu, X. Tang, E. F. Moore, and P. Chowdhury, Phys. Rev. C **76**, 054604 (2007).
[46] C. B. Wang, J. J. Zhang, Z. Z. Ren, and C. W. Shen, Phys. Rev. C **82**, 054605 (2010).